ELSEVIER

Thermochimica Acta 291 (1997) 117–130

thermochimica acta

Thermal analysis of fictile votive statues of 3rd century B.C.

Mauro Tomassetti[a,*], Luigi Campanella[a], Paola Flamini[a], Giovanna Bandini[b]

[a] *Department of Chemistry, University 'La Sapienza' P.zza A. Moro, 5, Rome 00185, Italy*
[b] *Museo Nazionale Romano, Rome, Italy*

Received 11 December 1995; received in revised form 22 July 1996; accepted 1 September 1996

Abstract

The potential of thermoanalytical techniques in the study of cultural assets and, in particular, the characterization of archaeological finds has been demonstrated in a number of publications appearing in international literature. This paper presents the results of thermoanalysis carried out to obtain a detailed characterization of several terracotta samples belonging to fictile statues of the 3rd–2nd century B.C., discovered in Ariccia (Rome, Italy). Thermoanalytical results, supported by X-ray diffractometry and IR-spectroscopy, are discussed in terms of the original assembly and firing of the archaeological finds and their subsequent restoration. The analytical methods used are also discussed here. © 1997 Elsevier Science B.V.

Keywords: Finds; Statues; Terracotta; Thermal analysis

1. Introduction

Thermoanalytical characterization of some small finds (each weighing only a few hundred milligrams) originating from different portions of votive statues found near Ariccia (Lazio) is presented in this paper. The Ariccia fictile material comprises several terracotta statues, slightly less than life-size, the most interesting of which depict a female figure seated on a throne (Figs. 1 and 2). Other materials consist of acephalous statues, e.g. those shown in Figs. 3005. All the finds have been dated as belonging to 3rd–2nd century B.C. because of the close resemblance to the heads and fictile votive masks of the republican 'stipi' of the people of Latium and of Latin origin [1]. Nevertheless, a broader middle Italic influence, which in that period was characterized by a strongly hellenized artistic culture [2], is more evident.

While there is no lack of studies on the stylistic and typological characterization of the finds, technological information is available concerning, for instance, the materials and the construction features of these terracottas. The available information refers essentially to the mineralogical phases present in these finds and is obtained by X-ray diffraction [3]. We recently subjected one of these statues to a brief investigation [4]. The examination of this single find nevertheless revealed quite clearly that, of all the analytical techniques used, thermoanalysis may be considered as playing a very important role. Furthermore, the importance of thermal analysis for pottery characterization had already been pointed out by Mackenzie [5]. The possibility of using thermomechanical analysis to estimate the firing temperature of pottery has been accurately documented, for example by Roberts [6]

*Corresponding author. Tel.: 0649913722 or 06 49913725; fax: 0649913725 or 06490631.

PII S0040-6031(96)03080-8

Fig. 1. Terracotta statues of the Ariccia fictile building. The analysed nine terracotta samples, are those belonging to the sites labelled with No. 1–9, respectively.

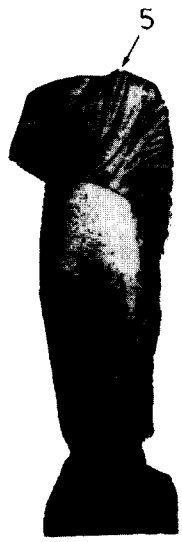

Fig. 3. Terracotta statues of the Ariccia fictile building. The analysed nine terracotta samples, are those belonging to the sites labelled with No. 1–9, respectively.

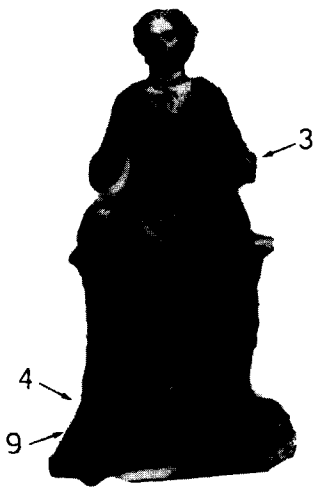

Fig. 2. Terracotta statues of the Ariccia fictile building. The analysed nine terracotta samples, are those belonging to the sites labelled with No. 1–9, respectively.

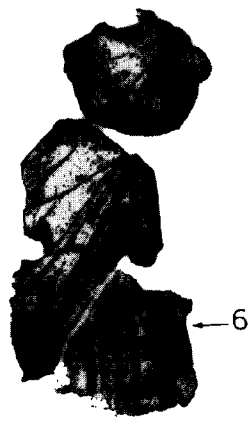

Fig. 4. Terracotta statues of the Ariccia fictile building. The analysed nine terracotta samples, are those belonging to the sites labelled with No. 1–9, respectively.

and Tite [7]. A very interesting application was recently proposed for this by Wiedemann [8], while Veniale [9] reported that the characterization of raw (secondary) phases in pottery can be improved by thermal analysis. Finally, Moropoulou et al. showed in a recent paper [10] how thermal analysis can be effectively used to characterize ancient ceramic technologies. With this in mind several terracotta samples taken from the more representative fictile statues from the Ariccia archaeological complex were subjected to

Fig. 5. Terracotta statues of the Ariccia fictile building. The analysed nine terracotta samples, are those belonging to the sites labelled with No. 1–9, respectively.

thermogravimetric (TG), differential thermal (DTA), differential scanning calorimetric (DSC) and thermomechanical (TMA) analyses. The same samples were also examined by X-ray diffraction (XRD) and infrared spectrometry (IR). The results of these tests, which afforded an exhaustive characterization of several of the most important finds from the archaeological complex investigated, are reported in detail herein. However, one of the aims of the present investigation was also to show how modern thermoanalysis instrumental techniques can provide significant information not only about the component materials of archaeological finds, but often also about the level of technology employed and in some cases also the nature of restoration interventions from previous periods, which are usually comparatively undocumented.

2. Experimental

2.1. Sampling, apparatus and methods

All the small terracotta finds examined came from fictile statues belonging to the 'Ariccia Plastic Group' preserved at the Museo Nazionale Romano (Rome). All nine samples, in the form of non- homogeneous fragments, were first carefully ground into homogeneous powder to be used in the various analyses.

The thermogravimetric analyses were performed using a Mettler TG 50 thermobalance; the calorimetric analyses were performed on a DSC 20 Mettler apparatus. Both instruments were connected to a TC 10 A microprocessor and a Swiss dot-matrix printer. The experiments were carried out at a heating rate of 10 and 5°C min^{-1}, respectively, and an air-flow rate of 100 cm^3 min^{-1}. The differential thermal analyses were carried out on a Du Pont apparatus (DTA cell) coupled to a thermal Analyst 2000 Du Pont system at a heating rate of 10°C min^{-1}. The thermomechanical tests were performed on a Mettler TMA 40 thermomechanical analyzer, coupled to the microprocessor and printer described above and used also for the TG and DSC tests. In this type of analysis the powdered terracotta samples were placed in cylindrical alumina sample-holders (5 mm in diameter and 5 mm high) equipped with an alumina piston capable of sliding inside the cylindrical sample holder and in close contact with the levelled-out surface of the sample. Above all the samples were subjected to an isothermal (25°C) recompaction process, repeated two or three times if necessary. This entailed applying a constant load of 0.4 N for 10 min on the piston together with a dynamic charge of 0.1 N (at a frequency of 5 cpm). At the end of this treatment the samples were subjected to thermodilatometric scanning between 25° and 1 000°C, in the same cylinder as described, at a heating rate of 8°C min^{-1}, in static air conditions and with a constant applied load of 0.05 N.

The TMA plots thus obtained are very similar to those found by Bayer and Wiedemann [11] using the same technique, although this time on Nabatean pottery samples that had not previously been powdered. This supports the belief that the recompacting treatment described here and used by us was largely successful in achieving the stated aim.

X-ray diffraction tests were performed on a PAD III Seifert automatic powder diffractometer using CuK_α radiation ($\lambda = 1.54$ Å).

IR spectrometric analyses were carried out using a Perkin–Elmer mod. 882 infrared spectrophotometer, with direct dispersion of the powder comprising the sample in KBr pellets.

3. Results

Figs. 1–5 show a front view of all the fictile statues examined. As can be seen, Figs. 1 and 2 refer to two very similar finds, each representing a female figure seated on the throne. Figs. 3–5 refer to three different acephalous statues. The analysed samples are indicated by numbers 1–9.

Figs. 6–8 show the TG and DTG curves, between 20° and 1000°C, for all the samples tested. The relevant thermogravimetric data, referring to the temperatures of the various steps and the loss of mass during the steps themselves, are recapitulated in Table 1. Fig. 9 shows the DTA curves between 30° and 1000°C, while Fig. 10 gives the more interesting DSC curves of some of the aforementioned samples between 20° and 400°C. Fig. 11 shows the TMA and DTMA curves of some of these samples between 25° and 1000°C, while the main thermomechanical results are set out in Table 2. Data from X-ray diffraction spectra of the fictile samples are shown in Table 3. The main minerals contained in the terracotta samples,

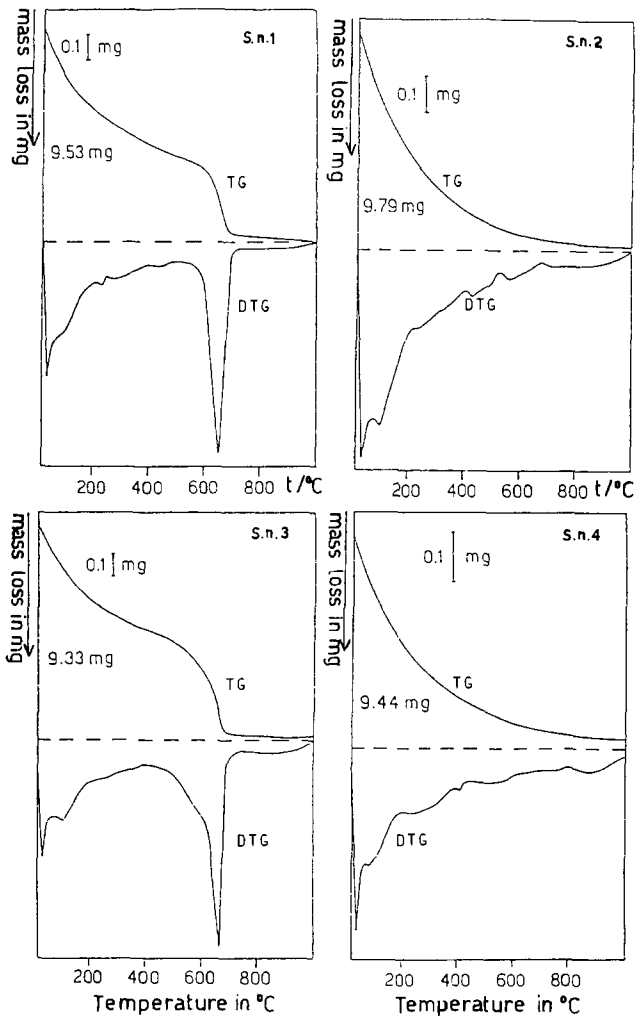

Fig. 6. TG and DTG curves for the characterization of terracotta sample Nos. 1, 2, 3 and 4, belonging to statues, represented in Figs. 1 and 2. TG in an air stream (100 cm^3 min^{-1}); heating rate 10°C min^{-1}.

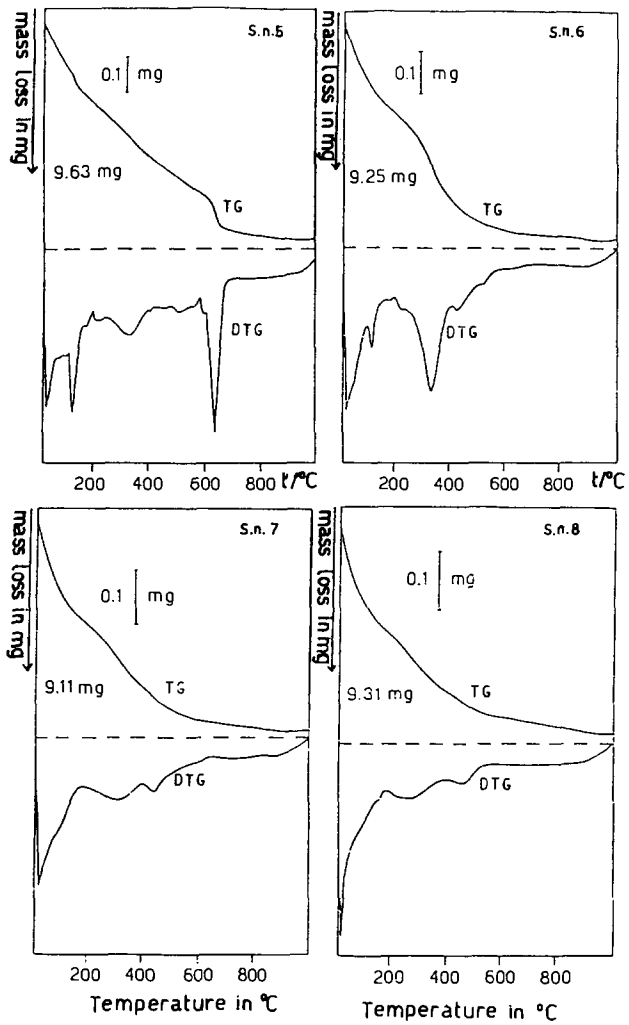

Fig. 7. TG and DTG curves for the characterization of terracotta sample Nos. 5, 6, 7 and 8, belonging to statues, represented in Figs. 3–5. TG in an air stream (100 cm^3 min^{-1}); heating rate 10°C min^{-1}.

identified using this technique, are indicated in this table. Lastly, the IR spectra for most of the samples, are set out in Fig. 12.

4. Discussion

As already mentioned, the thermogravimetric results are set out in Table 1. For the samples tested the main differences were found at temperatures around 500–750°C. At these temperatures a clear-cut thermogravimetric step occurs (Step e in Table 1), which emerges clearly in the TG and DTG curves of Samples 1 and 3 in Fig. 6 and, to a lesser extent, in the TG and DTG curves of Samples 5 and 9 (see Figs. 7 and 8). This step is not visible in the analogous thermogravimetric plots shown in Figs. 6 and 7 referring to Samples 2, 4, 6, 7 and 8, respectively. The TG curves of these latter samples generally display a percent residue at 1 000°C which is appreciably higher than that observed for samples showing this step (see Table 1). The thermogravimetric Step e is typical of

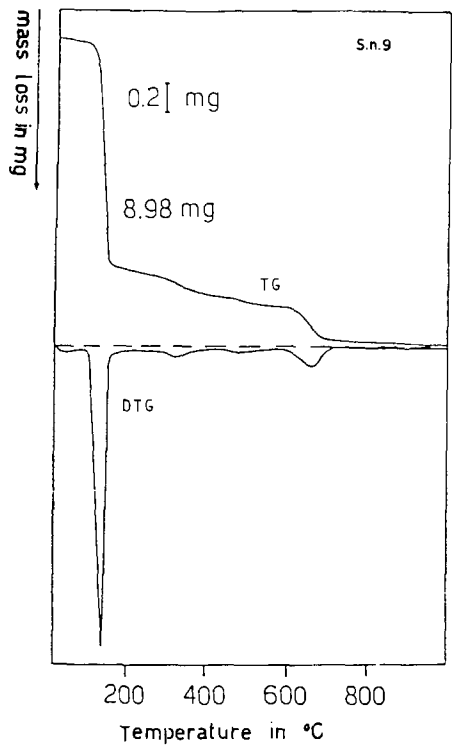

Fig. 8. TG and DTG curves for the characterization of terracotta sample No. 9, belonging to the statue, represented in Fig. 2. TG in an air stream (100 cm^3 min^{-1}); heating rate 10°C min^{-1}.

carbonate decomposition [12]. This is confirmed by the endothermic peak, determined at the same temperatures as in the DTG curves, observed in DTA curves of Samples 1, 3, 5 and 9 in Fig. 9, where all nine DTA curves, referring to the nine samples examined, are respectively plotted. Fictile Samples 1 and 3 contain a significant quantity of carbonate (4.4% and 7.4% by weight as CO_3^{2-}, respectively), mainly in the form of calcium carbonate (see X-ray diffraction spectrometry results and IR tests in the following). Samples 5 and 9 contain small amounts of carbonate (about 1.5% and 3.4% by weight as CO_3^{2-} respectively). In most other thermogravimetric steps shown in Table 1 and observable in the TG and DTG curves in Figs. 6 and 7, no significant differences among the samples were found. In particular, steps a and b, the peaks for which appear in the DTG curves respectively at around 23–90°C and 90–200°C, can definitely be attributed to the loss of moisture and hydroscopic bound water [10], retained by the fictile material. It follows that the total water contained in these two steps is around (2–3.5)% by weight in Samples 1–8, and around 17% by weight in Sample 9. Water loss for Samples 1–8 occurs in two steps – a faster one occurring at the lower temperature, i.e. about 23–90°C and a slower one peaking at around 100–130°C and ending at about 200°C. This is confirmed by the endothermic trends clearly visible in the DSC plots in Fig. 10. In this figure, the second TG step is seen to correspond generally to a large endothermic gap in the DSC curves, rather than to an actual endothermic peak, whereas, for Sample 9 only, two distinct endothermic peaks are observed at about 140° and 160°C, respectively. In the case of Step c of the thermogravimetric curves, to which corresponds a slight loss of mass (~ 1–2%), as shown in Tables 1 and 2, between ~ 200° and 450°C, slight, although tendentially exothermal, effects are observable both in the DTA curves and in the DSC curves. This exothermal effect is more evident in the DTA curves of Samples 6 and 9, which corresponds to a clearly marked thermogravimetric step in the respective TG and DTG curves of Figs. 7 and 8. The thermogravimetric Step c could thus reasonably be explained in terms of the oxidation and combustion of small quantities of organic substances present in the sample [13]. In this connection, it should be noted that the presence of small quantities of organic substance in these samples could not really be accounted for by the persistence of colour residues, albeit highly degraded, as the fictile statues were originally polychrome [2]. In fact, these colours were generally of an inorganic nature [14]. The small quantities of organic substance found could however be accounted for also in terms of microscopic residues of lichens [15] growing on the surface as a result of the damp environment surrounding the statue over the centuries.

Lastly, the thermogravimetric Step d is very small and thus not very significant. It can tentatively be ascribed either to the release of traces of the so-called structural bound water [9,10], i.e. the small amount of water originating from the loss under heating, of hydroxyl groups still present in some minerals [13], or else to the very slight traces of carbonates barely detectable in the DTA curves.

The TG and DTG curves of Sample 9, shown in Fig. 8, indicate that this sample, which was taken from

Table 1
Main thermogravimetric data of terracotta samples (1)—→(9). TG in an air stream (100 cm^3 min^{-1}); heating rate 10°C min^{-1}

	[a]		[b]		[c]		[d]		[e]		residue
Sample No.	weight loss (%)	pdt [a]	weight loss (%)	pdt [a]	weight loss (%)	pdt [a]	weight loss (%)	pdt [a]	weight loss (%)	pdt [a]	%
1	1.3	23	1.8	75	1.9	200			3.2	500	91.6
		35				280				640	
		75		200		500				750	
2	1.2	22	2.2	75	2.2	200	0.3	535			93.7
		38		90		450		560			
		75		200		535		695			
3	1.0	22	2.5	60	1.6	200			5.4	400	89.3
		33		105						665	
		60		200		400				750	
4	0.9	23	1.2	80	1.2	200	0.6	415			95.9
		33				250		510			
		80		200		415		690			
5	1.1	22	1.1	100	1.8	200	0.9	425	1.1	575	93.5
		30		130		325		510		635	
		100		200		425		575		700	
6	1.2	22	0.8	100	2.3	200	0.7	420			94.6
		30		120		330		430			
		100		200		420		650			
7	1.1	22	0.8	95	1.0	200	0.7	400			96.3
		30				320		450			
		95		200		400		650			
8	1.1	22	0.8	93	1.2	200	0.7	400			95.9
		30				320		450			
		93		200		400		650			
9	0.4	25	16.8	95	1.4	200	0.8	400	2.5	575	76.9
		55		135		325		470		660	
		95		200		400		575		730	

[a] 'Procedural decomposition temperature'.

the bottom portion of the throne of the statue depicted in Fig. 2, is very different from those described before; in fact, a very strong TG step, due to crystallization water loss, occurs between ~ 100° and 200°C. On the other hand, two large endothermic peaks are seen to correspond to this clear-cut step, both in the DTA and DSC curves of Sample 9. All these experimental facts are a sure indication that 80.3% (w/w) of gypsum [16,17] is contained in Sample 9. Examination of the TG and DTA curves of this sample also reveals a carbonate decomposition step (see Step e in Table 2); in addition, an exothermic peak in the DTA curve at ~ 330°C, already found in Sample 6, reveals the presence of traces of organic matter. Furthermore, it is not possible to rule out the presence in Samples 6 and 9 of very small traces of calcium oxalate, which apparently must ultimately be associated with the discovery of organic residues due to lichens [15].

Data obtained from the thermomechanical analyses of some of the terracotta samples are summed up in Table 2. The TMA and DTMA curves are shown in Fig. 11. At low temperatures, the plots of some of these curves display a slight initial downward trend that can reasonably be attributed, in part, to the crushing and homogenization pretreatments performed on the samples prior to analysis. The latter were probably not entirely compensated for by the recompacting procedure described in Section 2 (Experimental). Another partial explanation is perhaps linked to the loss of moisture present in the samples, which was also detected by means of thermogravimetric analysis. Therefore, starting from

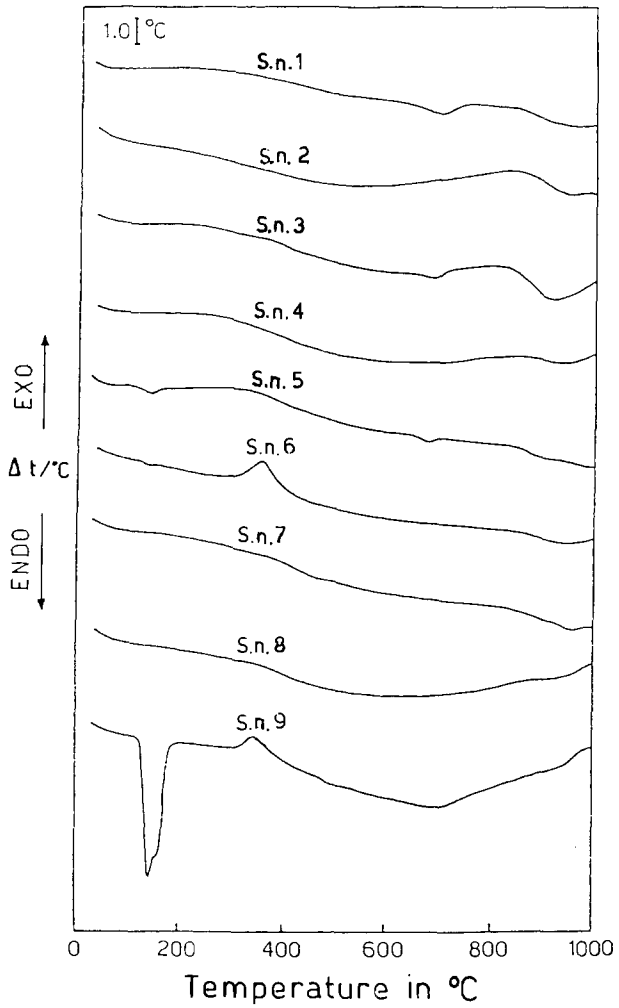

Fig. 9. DTA curves for the characterization of the examined terracotta sample Nos. 1–9; DTA in static air, heating rate 10°C min^{-1}.

~ 200°C, a slightly expansive process begins, which speeds up between ~ 500° and 650°C. This process has been divided into two steps in Table 2: a first, indicated as Step a, the upper limit of which is observed at ~ 550°C, can be ascribed to the rearrangement of a certain mineral crystal lattice [7], probably also due to a very small loss of structural bound water. The second expansion step (Step b) which occurs between ~ 550° and 650–700°C, above all can be attributed to the allotropic transformation of quartz from the α to the β form [8,13]. In the DTMA curve of Samples 2 and 4, the $\alpha \rightarrow \beta$ transformation of the quartz is more apparent than in the case of the equivalent curves for other samples (e.g. those for Samples 1 and 3).

At higher temperatures, up to ~ 650–750°C, the TMA curves display an almost horizontal trend and, lastly, a contraction process (Step c), which occurs either in a single stage, centred at ~ 870–880°C (see the DTMA curves in Fig. 11) or in two consecutive stages. The examined samples differ considerably as far as these latter TMA steps are concerned, since both steps correspond to carbonate decomposition and at the beginning of sintering processes in which the silica and alumina present react with other existing oxides to produce silico-aluminate complexes [13]. Indeed, in

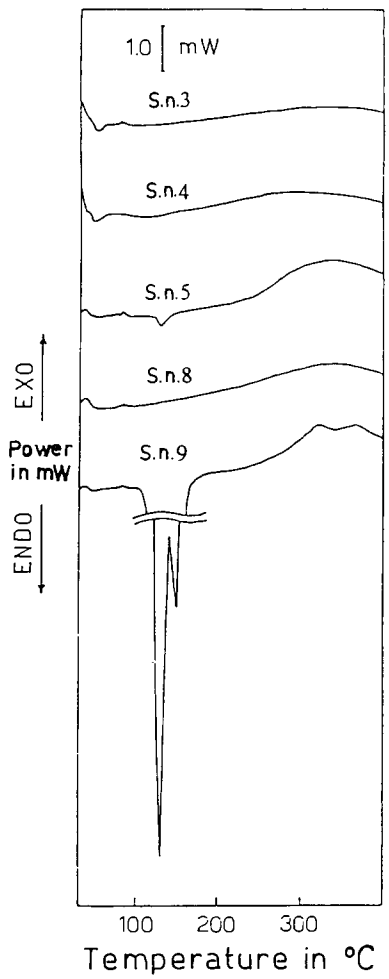

Fig. 10. DSC curves for the characterization of terracotta sample Nos. 3, 4, 5, 8 and 9. DSC in a air stream (100 cm^3 min^{-1}), heating rate 5°C min^{-1}.

some cases, the contraction process appears incomplete even at a temperature of 1000°C (the maximum temperature attainable with the TMA apparatus used by us). Table 2 also shows the firing temperatures estimated solely from the experimental value of the 'shrinkage temperature' (the temperature at which, once the expansion process is over, contraction begins) [6,7] and without using any corrective algorithm [7]. For this reason they may well prove comparatively inaccurate, as other authors [3] previously claimed that the firing temperatures of artifacts, like those examined by us, are generally lower than those found here using TMA. We have nevertheless reported the values found, even though they may be too high as absolute values, in order to show that, in any case, there appears to be a fairly considerable difference (at least 50–100°C or so) between the firing temperatures obtained for Samples 1 or 3 and Samples 2, 4, 5 and 8.

The diffraction spectra data [18] referring to the analysed samples shown in Table 3 confirm the results obtained using thermal methods, e.g. the presence of appreciable quantities of calcite only in Samples 1, 3 and 9 and smaller amounts in Sample 5 the presence of quartz, in varying percentages, in all the samples, except Sample 9, and the strong presence of gypsum in the last sample and in trace quantities in Sample 5. Furthermore, pyroxene anorthite and plagioclase are found in all Samples 1–8; traces of feldspar are found in Samples 3, 5 and 6; lastly, traces of hematite, though in very small amounts, occur in all the samples.

It was not however possible to reach any definite conclusions on the basis of the diffractometric data provided, e.g. the paragenesis of the ceramic body, also because our X-ray diffractometry equipment is essentially capable of providing only qualitative information. With only diffractometric information of this type available, it was not possible to make any reliable correlation, as was in fact done by several authors already cited above [9,10], between the crystalline phases present and firing temperature values obtained by thermoanalytical means or by thermomechanical measurement, or else with the type of atmosphere prevailing during the firing of the artifacts. All we can say is that the presence of the crystalline phases identified by us using X-ray diffraction is in reasonable agreement with the estimated firing temperatures. Furthermore, the repeated finding of plagioclase, anorthite and pyroxene could be an indication of the presence of an essentially reducing atmosphere during the firing process [10].

In the IR-spectra (Fig. 12), we mainly find the broad bands of water in the 3000–3800 cm^{-1} region, and silicate or sulphate [19] in the 850–1300 cm^{-1} region, as well as the carbonate band at ~1450 cm^{-1} [20] (see spectra of Samples 1 and 9).

In Fig. 12 the IR spectrum of Sample 9 is compared with that of pure gypsum; it is evident that the two spectra are identical with the exception of the carbonate band, which is clearly visible in the spectrum of Sample 9.

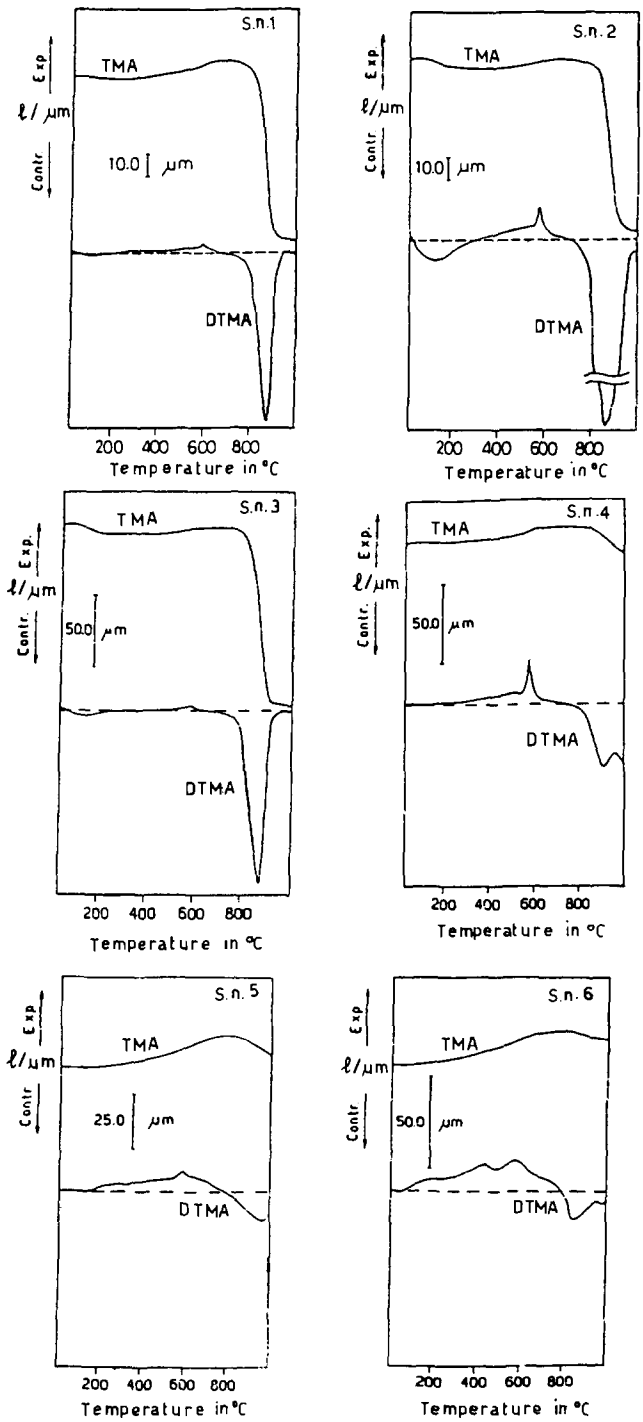

Fig. 11. TMA and DTMA curves for the characterization of terracotta sample Nos. 1, 2, 3, 4, 5 and 8, belonging to statues, represented in Figs. 1–3 and 5, respectively. TMA in static air; heating rate 8°C min^{-1}; applied constant load 0.05 N.

Table 2
Main thermomechanical data of terracotta samples belonging to statues of the Ariccia fictile building. TMA in static air; heating rate = 8°C min^{-1}; applied constant load = 0.05 N

	[a]		[b]		T_{eq} [b]	[c]	
Sample No.	expansion (%)	pt [a]	expansion (%)	pt [a]	(°C)	Shrinking (%)	pdt
1	+0.16	200	+0.11	520	655	−3.0	655
				575			875
		520		655			950
2	+0.02	150	+0.08	545	725	−3.1	725
				575			870
		545		725			990
3	+0.11	375	+0.09	560	660	−5.0	660
				575			870
		560		660			970
4	+0.16	200	+0.16	530	700	−0.6	700
				580			900
		530		700			970
5	+0.26	150	+0.18	550	760	−0.3	760
				575			860
		550		760			996
8	+0.22	200	+0.27	530	760	−0.3	760
				570			950
		530		760			995

[a] 'Procedural temperature'.
[b] 'Equivalent firing temperature', found on the basis of the experimental value of the 'shrinkage temperature' (T_a). Data are reported without further correction.

Table 3
Main data of X-ray powder spectra for terracotta samples. Principal minerals contained and semiquantitative extimation [a]

Sample No.	Calcite	Gypsum	Quartz	Ematite	Plagioclasium	Feldspar	Piroxene	Anortite
1	+++ [b]	+ [e]	++ [d]	+	+? [f]		++	+
2			+++	+	++		++	++
3	+++		++	+	++	+	+	+
4			+++	+	+		++	+
5	++	++	+++	++	+?	++	++	+++
6			+++	+	+++	+	++	++
7			+++	+	++		++	+++
8			+++	+	++		++	+++
9	+++	++++ [b]		+				

[a] Semiquantitative extimation performed on the basis of the number at d_{hkl} recovered and the intensity of relative peaks.
[b] Excess.
[c] Abundant.
[d] Present.
[e] Traces.
[f] Doubtful traces.

5. Conclusions

The results of the instrumental analysis described reveal a certain lack of homogeneity in the fictile material of which the entire statues are made and this is particularly evident in the case of two statues representing female figures seated on the throne (Figs. 1 and 2). In fact, Samples 1 and 3 have an easily detectable percentage of calcite, while Samples 2 and 4 are richer than the other two in silica (see TMA

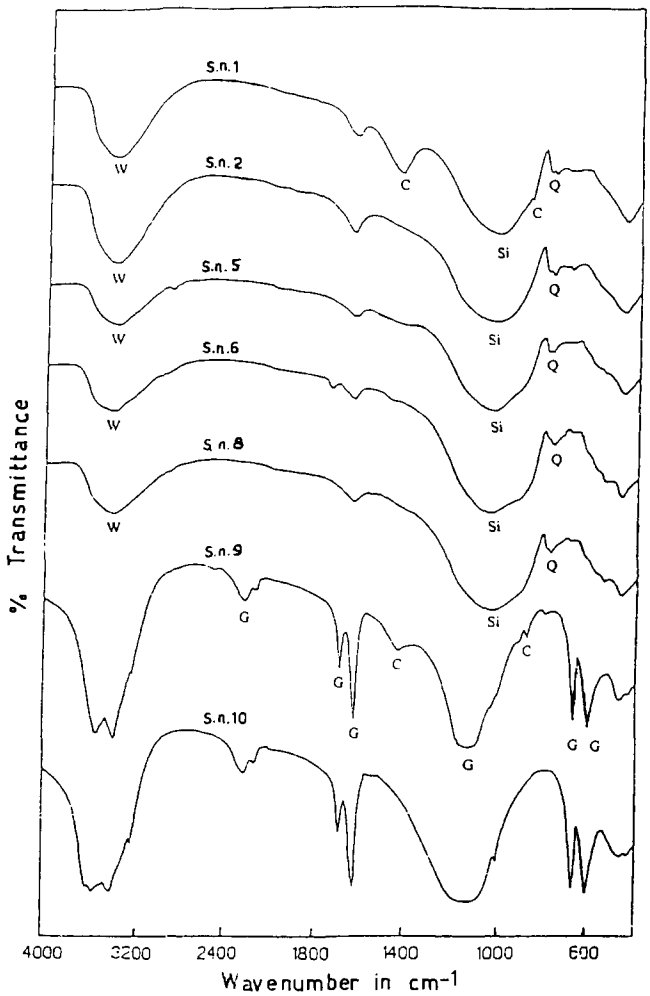

Fig. 12. IR spectra in KBr for the characterization of terracotta sample Nos. 1, 2, 5, 6, 8 and 9; Curve 10 standard of gypsum. Si: silicate; Q: quartz; C: calcite; G: gypsum; W: water.

curves). Lastly, the firing temperatures, as estimated from the trends of the thermodilatometric curves of Samples 1 and 3, are somewhat different (lower) from those of the other samples.

These differences may be explained in terms of several factors:

1. The technique used to manufacture the statue – in fact, the hypothesis previously advanced [1] that several parts of the fictile statue were made in separate moulds and then assembled to form a single complex before firing, seems to be confirmed.
2. The firing temperature does not seem to have been completely uniform – in particular, the base seems to have reached a higher temperature than the upper parts of the statues.

This is demonstrated both by the firing temperatures, as estimated by means of thermomechanical analysis, and the absence of calcite in samples belonging to the base of statues in Figs. 1 and 2, which would indicate a firing temperature certainly $\geq$ 700°C [12].

The significance of the experimental data obtained for the remaining three statues examined can be briefly summed up as follows: with reference to the statues

shown in Figs. 3 and 4, conclusions such as those drawn before for the statues in Figs. 1 and 2 may be partly applicable, even though the differences among the samples taken from the upper portion of the statues and those of the lower parts are less apparent in the case of the statues in Figs. 3 and 4 than for those in Figs. 1 and 2; also, the differences in the firing temperatures of the different parts seem to be smaller. Lastly, the statue shown in Fig. 5 seems to be the most homogeneous both as regards the materials used and the firing temperature (note, for instance, the absence of carbonates both in the sample taken from the upper portion and that from the lower part of the statue). Sample 9, taken from the lower part of the throne base of the statue in Fig. 1, represents a distinct case. The sample was probably removed from a previously restored portion of the statue; the presence of stucco repair work, already reported in various parts of these statues by other authors [2,3], would certainly account for the very high gypsum content found in this sample.

Lastly, several conclusions may be legitimately drawn concerning the analytical methods used. Thermal analysis techniques clearly played an important role throughout the investigation. The important results obtained, such as the differences detected in the material of which the various fictile statues were made or the differences between the upper and lower parts of them, or else the estimation of the firing temperature, or the detection of traces of a comparatively poorly documented restoration in one of the samples analysed, were all acquired by means of experimental measurements carried out using the classical thermal analysis techniques, namely TG, DTA, DSC and TMA. The other techniques used (IR-spectroscopy and X-ray diffractometry) usually confirmed the thermal analysis, often extending them, as in the case of X-ray diffraction of mineralogical characterization, but without introducing any significant novelties in the general framework of the research.

Acknowledgements

Research was carried out with the financial support of the National Research Council (CNR) of Italy.

References

[1] Assessorato Antichità Belle Arti e problemi della Cultura – X Ripartizione del Comune di Roma (ed.); "Roma Medio Repubblicana, Aspetti culturali di Roma e del Lazio nei secoli IV e III a.C.", De Luca (Publ.), Rome, Italy (1973) pp.312–327.

[2] M.R. Di Mino and M. Bertinetti (eds.), "Archeologia a Roma, la materia e la tecnica dell'arte antica", De Luca (Publ.), Rome, Italy (1990) pp.170–191.

[3] G. Guidi and A. Di Bartolomeo, in M.R. Di Mino and M. Bertinetti(eds.),"Indagini sul complesso fittile di Ariccia ed il gruppo del frontone di via S. Gregorio Roma", "Archeologia a Roma. La materia e la tecnica dell'arte antica", De Luca (Publ.), Rome (1990) pp.190–193.

[4] L. Campanella, G. Bandini, P. Flamini and M. Tomassetti Characterization of a fictile statue of the 3rd century B.C. by means of instrumental analysis, Sci. Technol. Cult. Heritage 3 (1994) 169–176.

[5] R.C. Mackenzie, Differential Thermal Analysis, 1 and 2, 1st edn., Academic Press, London (1970).

[6] J.P. Roberts Determination of the firing temperature of ancient ceramics by measurement of thermal expansion, Archaeometry 6 (1963) 21–25.

[7] M.S. Tite Determination of the firing temperature of ancient ceramics by measurements of thermal expansion: A reassessment, Archaeometry 11 (1969) 131–143.

[8] H.G. Wiedemann and G. Bayer Approach to ancient chinese artifacts by means of thermal analysis, Thermochim. Acta 200 (1992) 215–225.

[9] F. Veniale Clay science: Facts and perspectives, Miner. Petrog. Acta 35-A (1992) 13–43.

[10] A. Moropoulou, A. Bakolas and K. Bisbikou Thermal analysis as a method of characterizing ancient ceramic technologies, Thermochim. Acta 269/270 (1995) 743–753.

[11] G. Bayer and H.G. Wiedemann Thermoanalytical measurement in Archaeometry, Thermochim. Acta 69 (1973) 167–173.

[12] R. Grimshaw and A.B. Searle, The chemistry and physics of clays and other ceramics materials, E. Benn, London, UK (1959) pp.254–256.

[13] B. Fabbri and C. Fiori, Analisi termiche: Alcuni esempi applicativi nel settore dei ceramici tradizionali, in Caratterizzazione e reattività di materiali speciali, AICAT – IRTEC (CNR) (Publ.), Faenza, Italy (1990) pp.107–128.

[14] A. Ragona, Il rosso nella decorazione ceramica medioevale pugliese, Atti Convegno di ricerca storica, La ceramica in Puglia, Latiano, Brindisi (1983) p.57.

[15] H.G. Wiedemann and G. Bayer, Formation of Whewellite and Weddellite by displacement reactions, in: "Le pellicole ad ossalati: Origine e significato della conservazione delle opere d'arte", Proceedings, Milan, Italy, October 25–26 (1989) pp.127–135.

[16] G. Chiari, M.L. Santarelli and G. Torraca Caratterizzazione delle malte antiche mediante l'analisi di campioni non frazionati, Materiali e strutture II(3) (1992) 11–137.

[17] J. Paulik and M. Arnold Thermal decomposition of gypsum, Thermochim. Acta 200 (1992) 195–204.
[18] Powder diffraction file, in W.F. Mc Clune (Ed.),Search manual fink method, inorganic, and alphabetical index, inorganic materials, Int. Centr. Differ. Data (Publ.), Park lane, PA, 1978 and 1979..
[19] J.M. Hunt and D.S. Turner Determination of mineral constituents of rocks by infrared spectroscopy, Anal. Chem. 25(8) (1953) 1169–1174.
[20] M. Tomassetti, L. Campanella and G. D'Ascenzo Thermogravimetric analysis of conjugated and unconjugated sodium cholates, Thermochim. Acta 78 (1984) 235–249.